Molecular Crystals and Liquid Crystals Science and Technology. Section A. Molecular Crystals and Liquid Crystals
Publication details, including instructions for authors and subscription information:
http://www.tandfonline.com/loi/gmcl19

Multi-Photon Excitation and Relaxation of Thermal Gratings in the Nematic Liquid Crystal 5CB

H. J. Eichler [a] , R. Macdonald [a] & B. Trosken [a]
[a] Optisches Institut Technische Universität Berlin, Strasse des 17. Juni 135, D-1000, Berlin, 12, Germany
Version of record first published: 24 Sep 2006.

To cite this article: H. J. Eichler , R. Macdonald & B. Trosken (1993): Multi-Photon Excitation and Relaxation of Thermal Gratings in the Nematic Liquid Crystal 5CB, Molecular Crystals and Liquid Crystals Science and Technology. Section A. Molecular Crystals and Liquid Crystals, 231:1, 1-10

To link to this article: http://dx.doi.org/10.1080/10587259308032488

Mol. Cryst. Liq. Cryst., 1993, Vol. 231, pp. 1–10
Reprints available directly from the publisher
Photocopying permitted by license only

Printed in the United States of America

Multi-Photon Excitation and Relaxation of Thermal Gratings in the Nematic Liquid Crystal 5CB

H. J. EICHLER, R. MACDONALD and B. TRÖSKEN

Optisches Institut Technische Universität Berlin, Strasse des 17. Juni 135, D-1000 Berlin 12, Germany

(Received May 5, 1992)

We have observed strong thermal grating excitation in the isotropic and nematic phase of pentyl-cyanobiphenyl (5CB) in wave-mixing experiments using intense green picosecond excitation pulses at $\lambda_{exc} = 532$ nm. It is shown that optical heating is provided by a three-photon absorption process in the commonly called "highly transparent" liquid crystal. We have further investigated the relaxation of the induced thermal gratings, which exhibits a critical slowing at the nematic-isotropic phase transition.

1. INTRODUCTION

Laser-induced thermal birefringence changes in slightly absorbing nematic liquid crystals have been investigated as important optical nonlinear mechanisms beside the "giant"[1] reorientational nonlinearity in various experiments during the last years.[2,3,4] The observed large thermo-optic effects are, however, somewhat contradicted by a rather weak (linear) absorption for the most stable and applicable family of liquid crystals, the cyanobiphenyls, throughout the whole visible and near infrared spectral range. We have estimated e.g. the linear absorption of 5CB to about $\alpha_o = 10^{-2}$ cm^{-1} at $\lambda = 514$ nm. As a consequence, the absorption of these transparent materials has been often enhanced by adding appropriate dyes[3] or by coating the inner walls of the liquid crystal cell with absorbing layers[4,5] to obtain strong laser heating and the related thermal nonlinearity.

Recently, enhanced absorption without any additional absorbing material has been reported by Deeg and Fayer[6] who observed two-photon absorption and excited state gratings in wave-mixing experiments with 300 fs laser pulses in isotropic 5CB at $\lambda_{exc} = 575$ nm. It has been pointed out in this work, however, that the two-photon absorption is not sufficient to produce enough heat for the generation of strong thermal gratings, because the relaxation of the first excited singlet is mainly radiative. They conclude that at least a three-photon process may be responsible for heat generation.

In the present paper it is shown that strong thermal gratings in the nematic and

the isotropic phase of 5CB are generated by a three-photon process if short picosecond laser pulses at $\lambda_{exc} = 532$ nm are used. The observed nonlinear absorption is strongly anisotropic in the nematic phase. We have further investigated the thermal relaxation of the picosecond induced gratings on a microsecond time scale which exhibit a critical slowing behavior in the vicinity of the nematic-isotropic phase transition. Our experiments have been performed in a transient grating arrangement which is described in the following section 2. Theoretical considerations are given in section 3 and the experimental results are presented in section 4. Section 5 will finish the paper with concluding remarks.

2. EXPERIMENTAL SETUP

The experimental wave-mixing arrangement is sketched in Figure 1. Two 80 ps FWHM excitation pulses at $\lambda_{exc} = 532$ nm are obtained from a frequency doubled mode-locked Nd:YAG laser with a symmetric beam splitter. The linearly polarized beams are focussed to a diameter of 400 μm on a thin film of the liquid crystal 5CB which is temperature-controlled within ±0.1 K. Planar alignment of the nematic phase has been obtained by unidirectionally rubbing the inner glass surfaces of the container. The beams are crossed in the sample including an angle of 1 deg which results in an intensity grating with a fringe spacing of $\Lambda = 30$ μm. The polarization of the beams, the grating wave vector and the normal axis of the liquid crystal film are orthogonal to each other and may be labelled as the x-, y- and z-coordinate axis, respectively. The sample can be rotated around the z-axis to provide that the optical field is either parallel or perpendicular to the nematic director, the preferred axis of molecular alignment. This is important to avoid strong additional reorientation gratings which are usually observed in these experiments at arbitrary directions of the director with respect to the optical field.[7]

The absorbed intensity grating modulates the temperature and hence the birefringence of the fluid, and the centre of the resultant phase grating is probed by a weak argon cw-laser (488 nm) with a spot diameter of 100 μm. The first order diffracted probe beam intensity is measured with a photodiode and an oscilloscope. The scope traces are recorded with a digitizing video camera system.

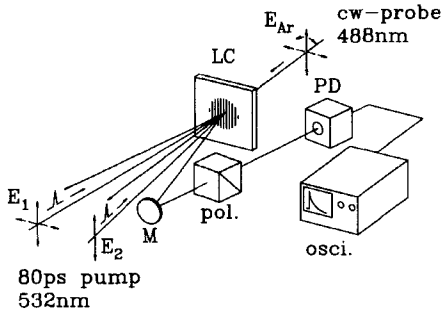

FIGURE 1 Experimental wave-mixing arrangement with LC:Liquid Crystal 5CB, PD: photodiode, M: Mirror, pol: Polarizer. E_1, E_2 and E_{Ar} are the optical fields of the pump and the probe beams, respectively.

3. THEORETICAL CONSIDERATIONS

If we consider two interfering laser beams which are slightly absorbed inside the liquid crystal film, the temperature rise due to laser heating can be described by the heat flow equation[8]

$$\frac{\partial T}{\partial t} - \text{div}(\underline{\underline{D}}\ \text{grad}\ T) = \frac{Q}{\rho c} \tag{1}$$

where T is the temperature, ρ the mass density and c the heat capacity. The heat production (per time and volume) Q is related to the absorbed input intensity and is discussed below. The heat diffusion in nematic liquid crystals can be described by a 2nd rank tensor $\underline{\underline{D}} = \underline{\underline{\lambda}}_w \rho^{-1} c^{-1}$ which is given by the heat conductivity tensor $\underline{\underline{\lambda}}_w$, the mass density ρ and heat capacity c.

In the present picosecond grating experiment the heat production can be assumed as spatially periodic and the solution of this equation in a plane wave approximation neglecting higher Fourier-components of the grating may be written as

$$\delta T = T - T_o = \frac{Q_o \tau_p}{\rho c} \exp\{-t/\tau\} \cos\{qy\} \tag{2}$$

where the thermal grating relaxation time $\tau = D_{\text{eff}}^{-1} q^{-2}$ contains the relevant (effective) heat diffusion coefficient and the grating wave number $q = 2\pi/\Lambda$. The heat production referring to the amplitude (peaks) of the induced grating is denoted as Q_o, τ_p is the laser pulse duration and T_o is the initial temperature. In evaluating Equation 2 we have assumed that the heat production is fast compared to the thermal relaxation times and that the main heat diffusion washing out the grating is from the peaks to the nulls of the grating.

In our experiments the effective heat diffusion coefficient D_{eff} is given by the two principal values $D_\perp$ and $D_\parallel$ in the nematic phase, where the indices refer to the coordinates perpendicular and parallel to the director, respectively, and by D_{iso} for the isotropic case. The two components of the nematic heat diffusion tensor are observed experimentally by applying the temperature gradient (i.e. the grating wave vector) perpendicular or parallel to the planar aligned director, respectively. Typical values for D_{eff} and τ are discussed below, together with the experimental results.

The heat production in the sample and thus the amplitude of the induced thermal grating at the beginning of the decay is determined by the absorbed intensity of the ps-excitation pulse. In many cases it is sufficient to use expressions[9] like $Q = \alpha I$ where α is the absorption coefficient and I the intensity, which implies, however, that the absorbed intensity is fast and completely dissipated as heat. Following the ideas of Deeg and Fayer[6] strong two-photon absorption (2PA) from the lowest energy band S_0 to the lowest excited singlet states S_1 can be expected in experiments with green intense laser pulses at $\lambda_{\text{exc}} = 532$ nm. The 2PA spectra essentially follows the one-photon absorption which peaks at $\lambda = 280$ nm in pure 5CB.[10] The 2PA probability is proportional to the number density of ground state molecules

and the photon density, i.e. the intensity. The absorption coefficient can be written in this case as $\alpha_{2PA} = \gamma_2 I$, where γ_2 is a constant. However, since the lifetime of the S_1-state is in the order of one nanosecond or somewhat less,[11] there is a strong probability that a third photon of the short picosecond laser pulse is absorbed by an excited state-excited state transition $S_1 \rightarrow S_2$. This additional one-photon absorption is very effective in our case, because the excitation pulse duration of about 80 ps is short compared to the S_1 lifetime, but large compared to the solvent cage reorganization time of 4 ps. The latter is important because the transition is shifted down to the excitation wavelength $\lambda_{exc} = 532$ nm by this process.[6]

The probability for the one-photon excited state absorption is proportional to the number density of singlet S_1 molecules which is proportional to the intensity absorbed by 2PA in our case, i.e. $\alpha_{12} = k\alpha_{2PA} I = \gamma_3 I^2$ where $\gamma_3 = k\gamma_2$ and k is a constant. The complete three-photon absorption process can then be described by the nonlinear absorption coefficient

$$\alpha = \alpha_{2PA} + \alpha_{12} = \gamma_2 I + \gamma_3 I^2 = \gamma_2 I(1 + kI) \tag{3}$$

The intensity independent S_0-S_1 one-photon absorption has been neglected because it is rather weak for our excitation wavelength as discussed above.

The heat production due to this nonlinear absorption is provided by fast radiationless recombination from the S_2 singlet states mainly and can be written as

$$Q = \alpha_{12} I = \gamma_3 I^3 \tag{4}$$

The temperature rise and the amplitude of the induced thermal grating can be calculated by using Equation 4 as a source term in Equation 2.

The birefringence and refractive index changes due to the temperature modulation are obtained with the optical dielectric tensor of the liquid crystal which can be written as[12]

$$\varepsilon_{\mu\nu} = \varepsilon_a a \left(L_\mu L_\nu - \frac{1}{3} \delta_{\mu\nu} \right) + \bar{\varepsilon} \delta_{\mu\nu} \tag{5}$$

where $\varepsilon_a = \varepsilon_{\parallel} - \varepsilon_{\perp}$ for perfectly aligned molecules, a is the scalar Maier-Saupe order parameter,[12] $L_\mu(L_\nu)$ are components of the director, the sum $\bar{\varepsilon} = \varepsilon_{\lambda\lambda}/3$ is the isotropic part of the dielectric tensor and $\delta_{\mu\nu}$ is the Kronecker-delta. The changes of $\varepsilon_{\mu\nu}$ due to the temperature rise are given by

$$\delta\varepsilon_{\mu\nu} = \left(\frac{\partial \varepsilon_{\mu\nu}}{\partial \rho} \frac{\partial \rho}{\partial T} + \frac{\partial \varepsilon_{\mu\nu}}{\partial a} \frac{\partial a}{\partial T} \right) \delta T \tag{6}$$

Using the Maxwell relation $n = (\varepsilon)^{1/2}$ for the refractive indices and the approxi-

mation $\partial\varepsilon/\partial\rho = (\varepsilon - 1)/\rho$ together with Equation 5 we obtain for the refractive index changes parallel and perpendicular to the director

$$\delta n_\perp = \left(\frac{n_\perp^2 - 1}{2n_\perp\rho}\frac{\partial\rho}{\partial T} - \frac{\varepsilon_a}{6n_\perp}\frac{\partial a}{\partial T}\right)\delta T \tag{7a}$$

$$\delta n_\parallel = \left(\frac{n_\parallel^2 - 1}{2n_\parallel\rho}\frac{\partial\rho}{\partial T} + \frac{\varepsilon_a}{3n_\parallel}\frac{\partial a}{\partial T}\right)\delta T \tag{7b}$$

which reduces to

$$\delta\bar{n} = \left(\frac{\bar{n}^2 - 1}{2\bar{n}\rho}\frac{\partial\rho}{\partial T}\right)\delta T \tag{7c}$$

in the isotropic phase.

The expressions between parentheses in Equations 7 are the relevant thermo-optic coefficients ($\partial n/\partial T$) which result from the temperature dependence of the order parameter a and the density ρ in the nematic phase, whereas the order parameter vanishes in the isotropic phase and laser heating leads to density changes only. We have neglected a coupling between the density and the order parameter in this treatment. Numerical values of the calculated thermo-optic coefficients can be estimated by using typical material parameters (e.g. at $|T - T_{NI}| = 10$ K) like $n_\perp = 1.53$, $n_\parallel = 1.74$, $\bar{n} = 1.66$, $a = 0.52$, $\varepsilon_a = 1.19$, $\{(\partial\rho/\partial T)/\rho\}_{iso} = -7.4\cdot10^{-4}$ K^{-1}, $\{(\partial\rho/\partial T)/\rho\}_{nem} = -8.2\cdot10^{-4}$ K^{-1} and $\partial a/\partial T = -7.2\cdot10^{-3}$ K^{-1} to $\partial n_\perp/\partial T = +5.7\cdot10^{-4}$ K^{-1}, $\partial n_\parallel/\partial T = -2.1\cdot10^{-3}$ K^{-1} and $\partial\bar{n}/\partial T = -3.9\cdot10^{-4}$ K^{-1} in good agreement with published data.[14]

The picosecond laser-induced refractive index changes and the resultant phase gratings are measured by diffraction of a probe beam in our experiments. The diffraction efficiency of a thin phase grating into the first order diffracted beam is given by[9]

$$\frac{I_1}{I_o} = |J_1(\delta\psi_o)|^2 \tag{8}$$

where J_1 is the first order Bessel function (of first kind) and $\delta\psi_o = 2\pi\delta n_o d/\lambda$ denotes the amplitude of the induced phase grating. I_1 is the first order diffracted intensity of a probe beam with an input intensity I_o. For weak gratings $\delta\psi_o << 1$ the approximation $J_1 = \delta\psi_o/2$ can be used and the diffraction efficiency depends on the square of the induced refractive index changes.

4. EXPERIMENTAL RESULTS AND DISCUSSION

Typical oscilloscope traces of the diffracted beam intensity as a function of time showing the grating decay are displayed in Figure 2. Since the magnitude of the

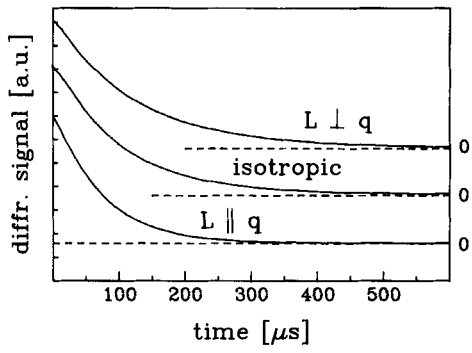

FIGURE 2 Thermal grating relaxation after 80 ps laser pulse excitation for nematic and isotropic 5CB at $|T - T_{NI}| = 10$ K.

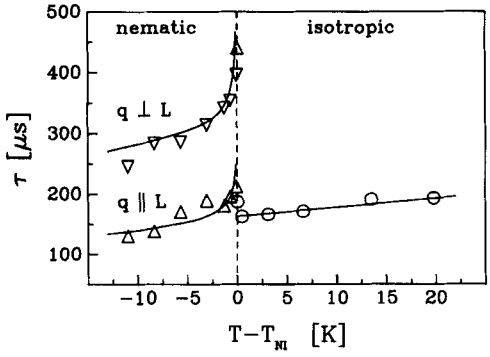

FIGURE 3 Thermal grating relaxation times as a function of temperature.

investigated thermal nonlinearity is different for the cases $L \| q$ and $L \perp q$ in the nematic phase and for the isotropic phase, the excitation energy was not the same for the three curves to obtain comparable diffraction efficiencies in the weak grating regime $\delta\psi << 1$. The signals almost show a single exponential decay in this case and the thermal relaxation time τ is simply two times the signal relaxation time because of the quadradic dependance between the diffraction efficiency and the grating amplitude. It should be noted, however, that this situation changes close to the phase transition at about $|T - T_{NI}| \leqslant 0.2$ K where the thermal grating decay is more wave-like rather than diffusive, leading to strong oscillations with a millisecond temporal periode. The origins of these oscillations are still under investigations and will be discussed elsewhere.

The evaluated thermal grating relaxation times range from 130 μs up to 450 μs depending on director orientation and temperature as depicted in Figure 3. There are two branches for τ in the nematic phase, corresponding to heat diffusion parallel or perpendicular to the director, showing a slower relaxation if the sample temperature is increased towards the nematic-isotropic phase transition. If the temperature is raised further, τ drops sharply down above the transition and then increases rather slowly in the isotropic phase. Typical values for the relaxation

times not too close to the phase transition (e.g. at $|T - T_{NI}| = 10$ K) are $\tau_\perp = 250\ \mu s$, $\tau_\parallel = 130\ \mu s$ and $\tau_{iso} = 180\ \mu s$ which can be explained by using the expression for the thermal relaxation time in Equation 2 with $q = 0.2\ \mu m^{-1}$ and heat diffusivities like $D_\perp = 0.9 \cdot 10^{-3}\ s^{-1}\ cm^2$, $D_\parallel = 1.8 \cdot 10^{-3}\ s^{-1}\ cm^2$ and $D_{iso} = 1.3 \cdot 10^{-3}\ s^{-1}\ cm^2$ in good agreement with published data.[14]

The observed temperature dependence of τ can be explained with the temperature dependence of the heat conductivity tensor and the heat capacity c at the first order nematic-isotropic phase transition,[15] whereas changes in the mass density are comparitively small and may be neglected in the following. If we rewrite the thermal diffusion time by using the expression for the heat diffusion coefficient as given together with Equation 1 we obtain $\tau = \rho q^2 c/\lambda_w$. The heat capacity c can be calculated by using the well-known thermodynamic relation $c = T(dS/dT)$ where the entropy $S = -(df/dT)$ is obtained from a Landau-type series expansion[12] of the free energy density f, which results in

$$c = \tilde{c}\{(1 - k(T - T_{NI}))^{-1/2} + 1\} \qquad \text{for } T \leqslant T_{NI} \tag{9}$$

where $\tilde{c}$ and k are constants. On the high-temperature side the critical increase of the heat capacity near the transition temperature is much less distinct[16] and c can be assumed constant for temperatures clearly above T_{NI} for our purpose. As a consequence the observed linear dependence of the thermal relaxation time in the isotropic phase is mainly a result of the temperature dependence of the isotropic heat conductivity $\bar{\lambda}_w$ which is fitted to our experimental data with

$$\bar{\lambda}_w = \frac{\rho c_{iso}}{q^2}\,(m(T - T_{NI}) + b)^{-1} \tag{10}$$

using[16] $c_{iso} = 1830\ JK^{-1}\ kg^{-1}$, $\rho = 1000\ kg/m^3$, $m = 1.5\ \mu s/K$ and $b = 163\ \mu s$. In addition we have the temperature dependence of the order parameter a influencing the anisotropy of the heat conductivity in the nematic phase. Using a similar expression like Equation 5 for the components of the heat conductivity tensor we get

$$\lambda_{w\parallel} = \bar{\lambda}_w + \frac{2}{3}\lambda_{wa} a \tag{11a}$$

$$\lambda_{w\perp} = \bar{\lambda}_w - \frac{1}{3}\lambda_{wa} a \tag{11b}$$

where the anisotropy $\lambda_{wa} = 0.410\ J\ (Kms)^{-1}$ can be evaluated from the experimental data $\tau_\perp/\tau_\parallel$ using Equation 10 together with an empirical expression[17] $a = (1 - 0.98\ T/T_{NI})^{0.22}$ for the order parameter. The change in the mass density at the nematic-isotropic phase transition has been neglected as mentioned above.

The remaining two parameters introduced with expression (9) for the nematic heat capacity are finally fit to the experimental data using Equations 10 and 11 to $\tilde{c} = 2.4 \cdot 10^3\ J/(K\ kg)$ and $k = 10\ K^{-1}$ which are close to values expected from

theory.[12] The agreement between the calculated and the measured relaxation times is quite good as shown in Figure 3 although we have used a simple Landau theory and a "classical" exponent 1/2 to describe the increase of c at the nematic-isotropic phase transition.

The investigated thermal gratings are excited by nonlinear absorption of the cyanobiphenyl molecules as discussed above. Strong gratings with saturated diffraction efficiencies up to 30% have been observed with isotropic samples, which is very close to the theoretical maximum of 34% for thin phase gratings.[9] Using nematic films, however, maximum "pure" thermal grating diffraction efficiencies up to 10% have been obtained, which are unlikely accompanied by additional reorientation effects in trying to exceed this value. As a consequence evaluation of the thermal grating amplitude is somewhat restricted to weaker gratings with nematic samples. In Figure 4 we have plotted the induced phase grating amplitude $\delta\psi_o$ as a function of excitation energy on a logarithmic scale, which has been evaluated with Equation 8 from diffraction efficiency measurements displayed in the inset of the same figure. The experimental data fit quite well to a cubic law which is a strong indication that the three-photon absorption process described in expression 4 is mainly responsible for the heat production. The temperature rise and thus the refractive index change (Equations 2 and 7c) is proportional to Q and therefore depends on W_p^3 in this case, whereas e.g. laser heating due to one-photon or 2P-absorption would result in a linear or quadratic dependence, respectively. The isotropic heat production coefficient obtained from these measurements using Equations 2, 4 and 7c together with the numerical values discussed above is given by $\bar{\gamma}_3 = 3.7 \cdot 10^{-25}$ m^3/W^2 and $k = 1.23 \cdot 10^{-13}$ m^2/W. The relative anisotropic nematic values are obtained to $(\gamma_3)_\perp = 0.14\ \bar{\gamma}_3$ and $(\gamma_3)_\parallel = 1.8\ \bar{\gamma}_3$.

Nonlinear absorption of the cyanobiphenyl molecules of course leads to nonlinear transmission of the samples which can be easily observed with thicker liquid crystalline films. In Figure 5 we have plotted the transmitted as a function of the incident pulse energy observed in single beam experiments with nematic films of 200 μm thickness. The experimental data clearly indicates a nonlinear transmission which can be explained by numerically solving the usual differential equation for

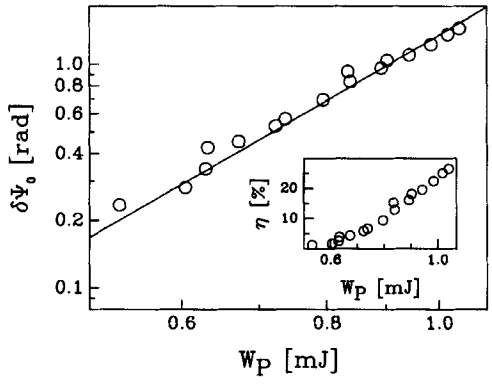

FIGURE 4 Evaluated thermal grating modulation-depth vs. excitation energy for isotropic 5CB. The inset shows the measured diffraction efficiencies.

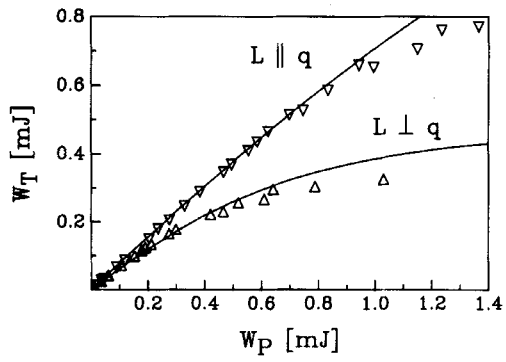

FIGURE 5 Nonlinear transmission of single beam 80 ps laser-pulses in nematic 5CB of 200 μm thickness.

the transmitted intensity using the nonlinear absorption coefficient introduced in Equation 3. Additional linear losses of $V_\perp = 20\%$ and $V_\parallel = 40\%$ due to scattering and interface reflections are also considered. To fit the experimental data we used the 2PA-coefficient $\gamma_2 = 3 \cdot 10^{-12}$ m/W from Reference 5 together with values γ_3 obtained from our thermal grating diffraction efficiency measurements discussed below. The anisotropic nematic 2PA-coefficient, however, is not known and can not be separated or determined from our experiments because of the large probability for the 3P-process, as mentioned above. Nevertheless, the agreement between the theoretical curves and experimental data is acceptable with respect to uncertainties of about 10% in the evaluated absorption coefficients.

Clearly the whole three-photon process and the resultant nonlinear transmission is anisotropic in the nematic phase with stronger absorption parallel to the director, in agreement with the results from heat production measurements. This is not surprising since the involved S_0-S_1 transition is polarized along the long molecular axis.

5. CONCLUSION

Excitation and relaxation of picosecond laser-induced dynamic thermal gratings has been investigated in the nematic and isotropic phase of the liquid crystal 5CB. It is shown that opto-thermal grating excitation is provided by heating due to a nonlinear three-photon absorption process if intense 80 ps laserpulses in the green spectral range at $\lambda_{exc} = 532$ nm are used. The nonlinear absorption is clearly anisotropic in the nematic phase, being stronger if the polarizations of the excitation beams are parallel to the preferred molecular alignment and weaker for perpendicular polarizations. For applications of liquid crystals in connection with short intense laserpulses it therefore may be important to use different wavelengths and/or other liquid crystals with different UV-absorption bands, if this nonlinear absorption is intolerable.

Relaxation of the induced thermal gratings is due to thermal diffusion not too close to the nematic-isotropic phase transition and has been investigated as a func-

tion of temperature and for different grating orientations. A critical slowing down has been observed for the thermal relaxation times in the vicinity of the phase transition temperature on the low temperature side. The observed temperature behavior of the relaxation is explained by the temperature dependence of the heat capacity and the anisotropic heat conductivity at the week first order phase transition. The increase of the heat capacity has been calculated from a simple Landau-theory resulting in good agreement between experimental and calculated relaxation times.

Acknowledgment

Financial support from the Deutsche Forschungsgemeinschaft via the "Sonderforschungsbereich 335 Anisotrope Fluide" is gratefully acknowledged.

References

1. N. V. Tabiryan and B. Y. Zel'dovich, *Mol. Cryst. Liq. Cryst.*, **62**, 637 (1981).
2. H. Hsiung, L. P. Shi and Y. R. Shen, *Phys. Rev. A*, **30**, 1453 (1984).
3. I. C. Khoo and R. Normandin, *IEEE J. Quant. Electron.*, **QE-22**, 329 (1985).
4. A. D. Lloyd, I. Janossy, H. A. MacKenzie and B. S. Sherrett, *Opt. Commun.*, **61**, 339 (1987).
5. R. Macdonald, J. Schwartz and H. J. Eichler, *Int. J. Nonl. Opt. Phys.*, **1**, 103 (1992).
6. F. W. Deeg and M. D. Fayer, *J. Chem. Phys.*, **91**, 2269 (1989).
7. H. J. Eichler and R. Macdonald, *Phys. Rev. Lett.*, **67**, 2666 (1991).
8. H. J. Eichler and H. Stahl, *J. Appl. Phys.*, **44**, 3429 (1973).
9. H. J. Eichler, P. Günter and D. W. Pohl, "Laser-Induced Dynamic Gratings," Springer Series in Optical Sciences 50, Springer Berlin (1986).
10. S. T. Wu and E. Ramos, *J. Appl. Phys.*, **68**, 80 (1990).
11. C. David and D. Baeyens-Volant, *Mol. Cryst. Liq. Cryst.*, **59**, 181 (1980).
12. S. Hess, *Z. Naturforsch*, **31a**, 1034, 1507 (1976).
13. W. Maier and A. Saupe, *Z. Naturforsch*, **14a**, 882 (1959) and W. Maier and A. Saupe, *Z. Naturforsch*, **15a**, 287 (1960).
14. I. C. Khoo, "Nonlinear Optics of Liquid Crystals," Progress in Optics, 26, ed, by E. Wolf, North-Holland Amsterdam (1988).
15. W. Urbach, H. Hervet and F. Rondelez, *Mol. Cryst. Liq. Cryst.*, **46**, 209 (1978).
16. J. Thoen, Preprint.
17. W. H. DeJeu, "Physical Properties of Liquid Crystalline Materials," Gordon and Breach, New York, (1980).